COUPLING BEHAVIOR OF SOIL STIFFNESS, EXCESS PORE WATER PRESSURE, AND STRAIN OBSERVED FROM DOWNHOLE ARRAY MEASUREMENT

C.C. Tsai[(1)], T. Kishida[(2)]

[(1)] *Professor, National Chung Hsing University, tsaicc@nchu.edu.tw*
[(2)] *Assistant Professor, Khalifa University of Science and Technology, tadahiro.kishida@ku.ac.ae*

Abstract

Geotechnical strong-motion downhole arrays, composed of strong-motion accelerometers distributed vertically throughout a site, provide engineers and seismologists with important data for identifying the dynamic response of a site as waves propagate through the subsurface. In this study, we analyze wildlife liquefaction array using the Normalized Input-Output Method (NIOM) to identify variations in shear wave velocity (Vs) and compression wave velocity (Vp) during strong motions. Variations in strain development with time in different azimuthal directions are also investigated. Once the induced shear strain exceeds the threshold strain (~0.01% as observed in this study), the excess pore water pressures (EPWPs) start accumulation. Prior to huge accumulations of EPWPs, the degradation of Vs is correlated to the magnitude of induced strain that is orientation-dependent. By contrast, as more EPWPs accumulated, EPWPs dominate the Vs degradation that become orientation-independent. On the other hand, even significant degradation of Vs is observed, only slightly degradation of Vp is observed. These behaviors need to be considered in the effective stress site response analysis.

Keywords: Downhole array; shear wave velocity; compression wave velocity; excess pore water pressures; strain

Introduction

Site response analysis is commonly used to account for local site effects on the surface ground motion. The effective-stress site response analysis is often considered to be a better approach because it is capable of modeling generation of excess PWP and associated cyclic softening to account for the reduction in soil stiffness during ground motion propagation. However, simultaneous numerical prediction of wave propagation, generation and redistribution of excess pore water pressures, and the resulting deformations remains challenging even under relatively simplistic level-ground free-field conditions (e.g. uniform properties within each soil layer and one-dimensional (1D) horizontal shaking). Furthermore, most efforts in the past have focused on the calibration and validation of constitutive model and numerical platforms with a given set of laboratory tests.

Geotechnical strong-motion downhole arrays, composed of accelerometers distributed vertically throughout a site, provide engineers and seismologists with important data for better understanding the dynamic response of a site as waves propagate through the subsurface. In this study, we compute shear wave velocity (Vs) and compression wave velocity (Vp) during strong motions for wildlife liquefaction array using the Normalized Input-Output Method (NIOM) (Haddadi and Kawakami 1998). Variations in strain development with time in different azimuthal directions are also investigated. The downhole arrays also provide the pore-water pressure measurements during strong motions. By comparing these information, the dynamic behavior of soil such as coupling of soil stiffness, PWP and strain level are investigated. The finding can be used as a basis to improve the 1D effective-stress site response analysis.

Methodology and Analyzed data

Methodology

This study downloaded three-component acceleration time series and pore-water pressure measurements from Wildlife arrays. The data before 2004 was obtained from COSMOS Strong-Motion Virtual Data Center (https://strongmotioncenter.org/vdc/scripts/default.plx) at the station NP.5210, where the data after 2004 are downloaded from NEES@UCSB (http://nees.ucsb.edu/data-portal) at the station of SB.WLA. From these recordings, the stain time series and wave velocities between downhole sensors are computed.

Figure 1a shows the flowchart of the data processing methodology used in this study. Two-component horizontal acceleration time series were rotated to the specified azimuthal angles. Shear-wave (Vs) travel times between downhole sensors were calculated by Normalized Input-Output Method (NIOM) following past studies (Haddadi and Kawakami 1998, Kishida et al. 2018). Figure 1b presents the methodology utilized to compute the displacement time series by applying filters and baseline corrections (Chiou et al. 2008, Ancheta et al. 2013). High- and low-pass acausal Butterworth filters were applied in the frequency domain with the corner frequencies of 0.2 Hz and 80% of Nyquist frequency, respectively. The shear strain (γ) time series are computed by subtracting displacement time series divided by the separation distances between sensors. The resulted γ was considered reliable when the period of γ obtained by the zero-crossing method was longer than 4 multiplied by the separation distance between sensors divided by Vs, where a similar control was suggested by Lysmer et al. (1975) for dynamic finite element analysis.

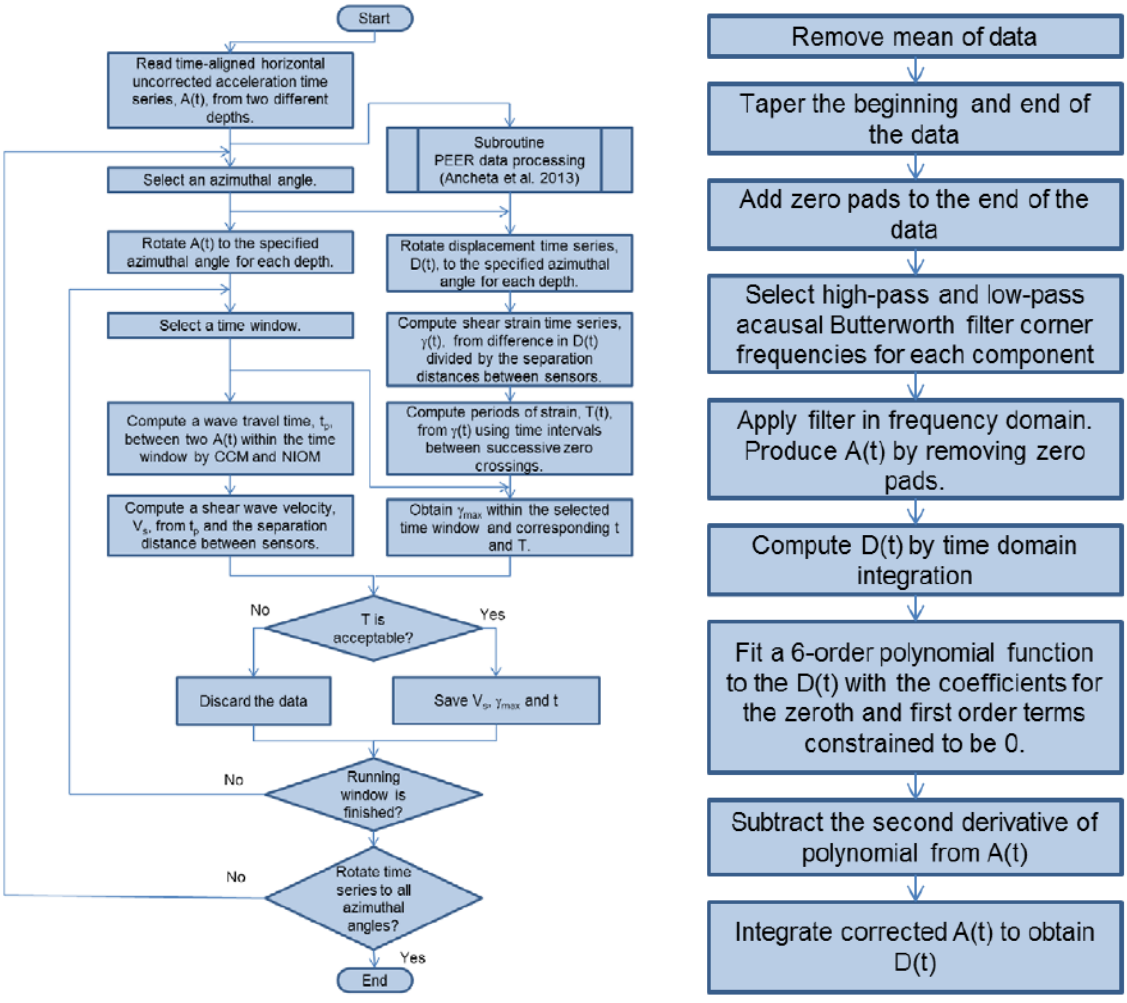

Figure 1 Flow chart of data processing method of (a) wave velocities (b) strain time series

Wildlife array

The Wildlife Array was established in 1982 on a floodplain in the Imperial Valley of Southern California, wherein sand boils developed during the 1981 Westmorland earthquake. The near-surface geology of the Wildlife site is composed of a 2.5 ~ 3.0 m thick layer of silty clay to clayey silt that caps the site. This layer is underlain by a 3.5 ~ 4.0 m thick layer composed of silt, silty sand, and sandy silt which is highly susceptible to the increase in pore pressure and potential liquefaction (Bierschwale and Stokoe 1984). This silty sand layer is underlain by a thick silty clay to clay layer. The arrays have 9 and 10 of accelerometers and pore water pressure transducers from 0 to 100 and 0 to 6.23 m depth, respectively. The accelerometers located at ground surface and at the depth of 7.7 m beneath the liquefiable layer) are analyzed. In addition, pore water pressures are obtained within the liquefiable layer. The locations ID of analyzed data are recorded at 04, 00, and 60-63, respectively. The horizontal separation distances between these locations are 8 m. Table 1 lists analyzed ten events recorded at Wildlife array. Peak ground acceleration (PGA) ranges from 0.09 to 0.31g. Moment magnitude (**M**) ranges from 3.2 to 7.2. The records of Superstition Hill event indicate the site was liquefied during the strong shaking. In this rest of the events, the site was not liquefied.

Table 1 Analyzed earthquake events for Wildlife Arrays

Event Name or Event ID	Origin Time (UTC)	Magnitude (**M**)	Hypocentral distance (km)	PGA (g) (NS, EW, UD)
Elmore Ranch	1987-11-24T01:54:16	5.9	23	(0.128, 0.128, 0.180)
Superstition Hills	1987-11-24T13:15:56	6.5	31	(0.205, 0.183, 0.423)
14607652	2010-04-04T22:40:43	7.2	100.5	(0.103, 0.139, 0.056)
15199681	2012-08-26T19:31:22	5.4	9.2	(0.136, 0.168, 0.329)
15200401	2012-08-26T20:57:57	5.5	8.8	(0.183, 0.181, 0.202)
15200489	2012-08-26T21:15:29	4.1*	6.8	(0.120, 0.080, 0.043)
15201537	2012-08-26T23:33:25	4.6*	7.7	(0.274, 0.279, 0.079)
15202921	2012-08-27T04:41:36	4.5*	8.6	(0.255, 0.313, 0.168)
15203249	2012-08-27T06:31:27	3.4**	6.0	(0.089, 0.042, 0.039)

*Magnitude is m_b. **Magnitude is M_L.

Analysis Results

Figure 2 to Figure 6 show the time series of (a) acceleration at ground surface, (b) acceleration at downhole, (c) pore-water pressure ratio (r_u) at the top of liquefiable layer, and (d) identified Vs time history as well as γ amplitudes between downhole arrays. No pore water pressure measurement was recorded in the Elmore Ranch event.

The identified Vs from Figure 2d – 6d are around 140 m/s prior to the strong shaking, which is consistent with the Vs measured by the field test (Bierschwale and Stokoe 1984). The Vs decreases due to large-strain level during the strong shaking with the generation of excess pore water pressure. In the 14607652 event (Figure 2), Vs decrease slightly due to a large strain at 50 sec (Figure 2d) while r_u remains very small. The Vs quickly increases back to the original value right after the strong shaking. In the 15201537 event (Figure 3), the Vs decease due to the strong shaking (induced $\gamma = 0.1\%$) at 20 sec. Moreover, it is interesting to observe that the Vs remains lower than 120 m/s even after strong shaking while r_u does not dissipated. Similar observation can be found in the 15202921 event (Figure 4). The Vs deceases at 15 sec while the

strain level increases to 0.08 % and Vs remains lower than 120 m/s even after strong shaking. In the Superstition Hill event (Figure 5), the site was liquefied at around 40 sec when r_u reaches 1.0 (Figure 5c) with a large strain induced (Figure 5d). Vs of the liquefied soil is around 20 m/s. Similar to the other events, Vs remains low (< 40 m/s) after strong shaking due to the remaining high r_u. By reviewing Figures 2-6, it was observed that the pore water pressure starts to increase when the γ amplitude exceeded 0.013% in average. This is consistent to the threshold strain observed in the laboratory experiments (Vucetic and Dobry 1986)

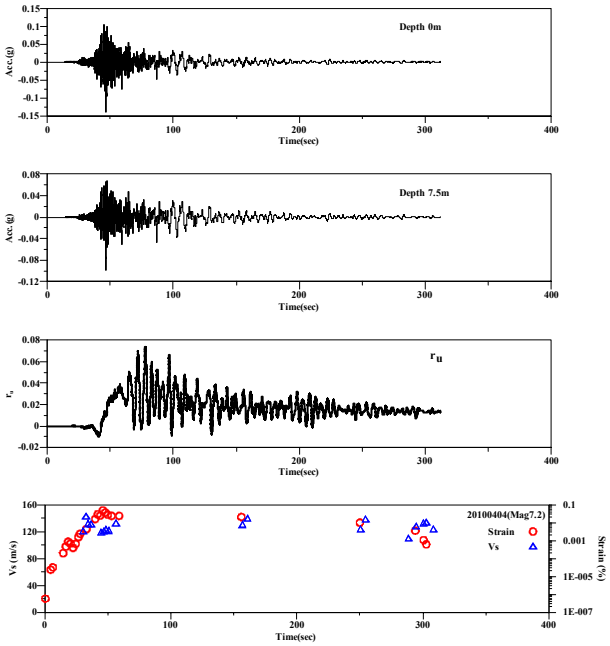

Figure 2 Recording and identified Vs and strain of 14607652 event

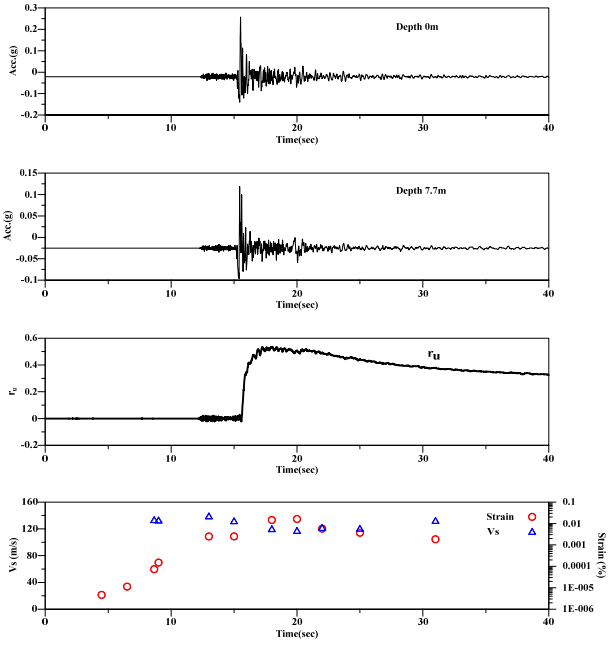

Figure 3 Recording and identified Vs and strain of 15201537 event

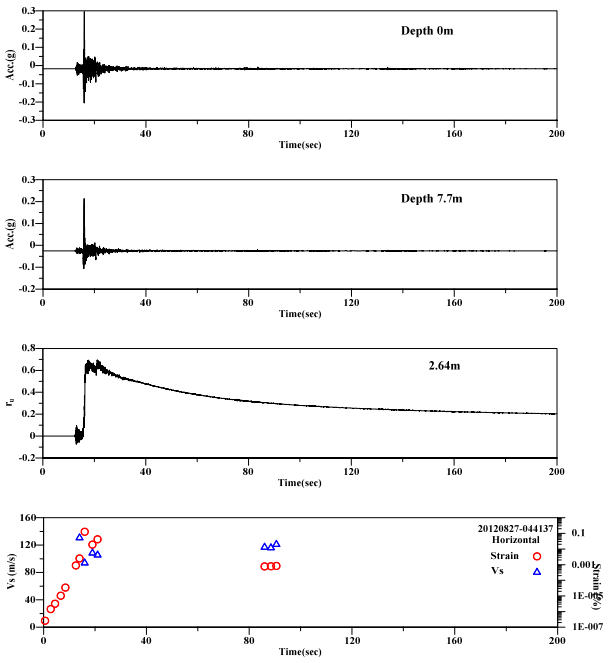

Figure 4 Recording and identified Vs and strain of 15202921 event

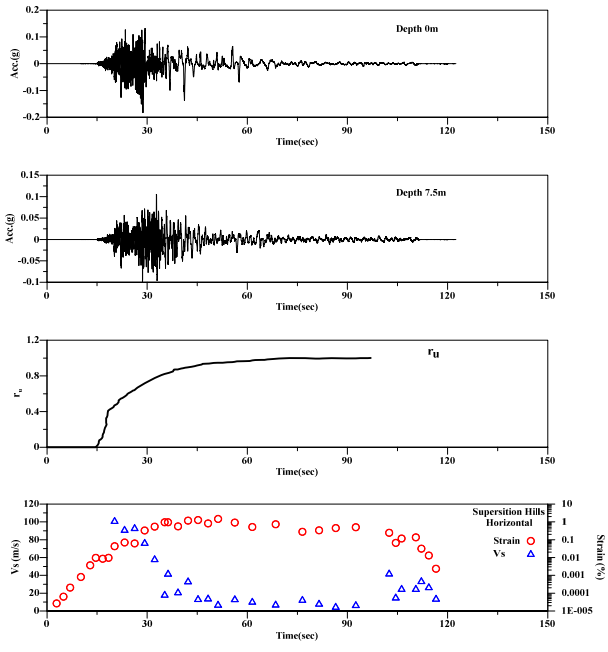

Figure 5 Recording and identified Vs and strain of Superstition Hill event

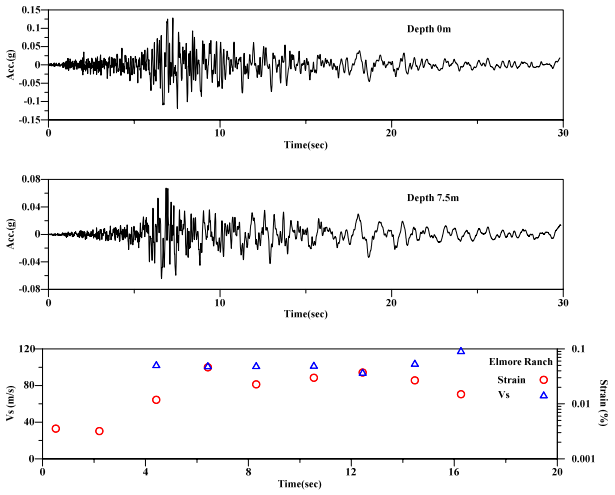

Figure 6 Recording and identified Vs and strain of Elmore Ranch

Figure 7 shows the identified Vs vs. γ of different orientations and different time windows. Generally, a higher strain leads to a lower Vs and vice versa. Because the strain levels are different at different orientations and consequently the Vs is expected to be different at different orientations, so called orientation-dependent behavior. Prior to the significant r_u (left figure), this orientation-dependent behavior is obvious because a clear trend of Vs decreasing with γ exhibits. However, as the r_u increases (right figure), a large scatter of Vs vs. γ is obtained. This is because Vs is not only related to the induced strain level at different orientations but also the r_u and thus the orientation-independent isotropic influence of pore water pressure becomes dominating.

Figure 8 shows a good example of orientation-dependent behavior prior to the r_u accumulation. The window of 14-16 sec exhibits the orientation-dependent behavior that a higher strain leads to a lower Vs in the corresponding direction. However, in another time window where encounters significant r_u, it is observed that the orientation-independent behavior that Vs remains similar even the strains are different in the different directions. This is because the Vs becomes controlled by r_u that is orientation independent.

Base on this observation, r_u needs to be estimated accurately in order to model the degradation of stiffness. In the 1D site response analysis, the horizontal component of ground motion (i.e. NS and EW) are typically propagated through soil column individually. For the condition without significant r_u, the approach is valid since the strain level dominates the degradation of Vs and can be estimated from each direction directly. However, as r_u increases, the orientation-dependent behavior omits, ideally, two components of motions need to be analyzed simultaneously. However, due to the limitation of current practice of site response analysis, the strongest azimuth of motions is suggested to be analyzed because r_u might be associated with the strain level estimated from the strongest azimuth. The obtained r_u by this manner is more accurate and can be used for the prediction of site response in all azimuth.

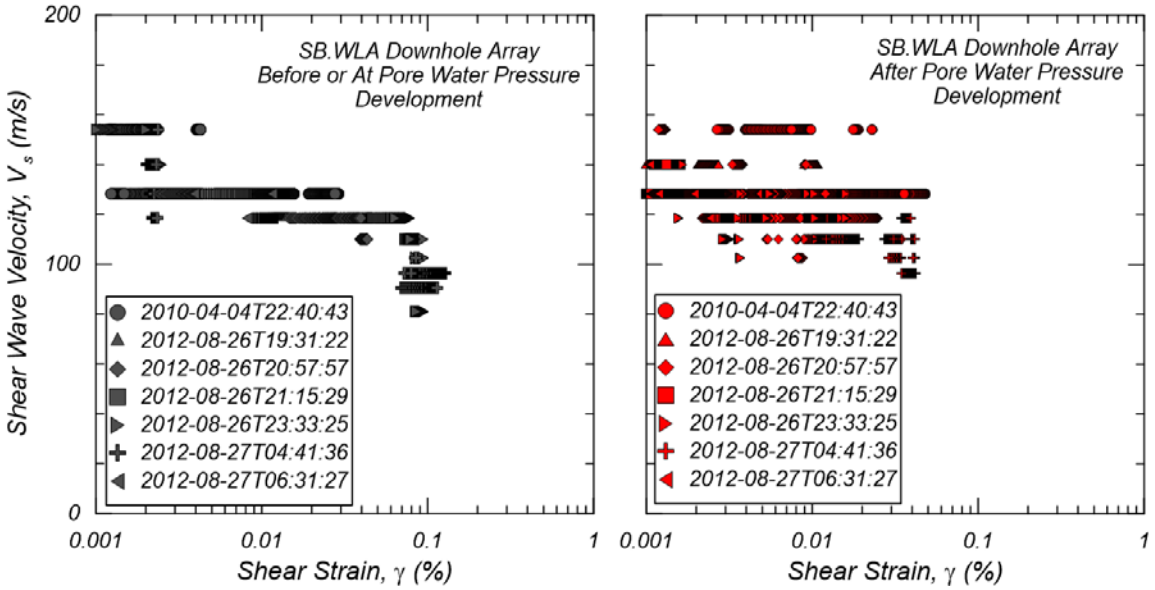

Figure 7 identified Vs vs. strain of different orientations and time windows prior and after PWP development.

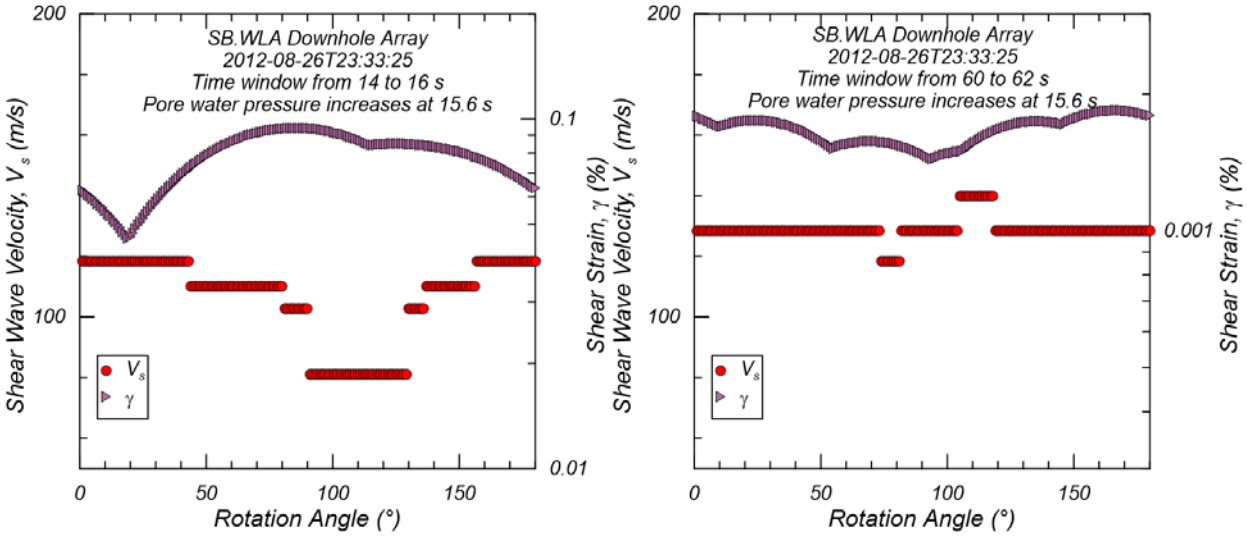

Figure 8 identified Vs and strain of different orientation prior and after PWP development. (15201537 event)

Figure 9 to Figure 11 shows the identified Vs and Vp time history as well as strain history of each event. It should be noted that the identified Vp oscillates between 1xVp and 2xVp (e.g. 800 m/s and 1600 m/s in 15200401 event, Figure 10), This is due to the limitation of data resolution (i.e. sampling frequency) given the separation distance between surface and downhole measurement. The actual Vp could be any value in between. Therefore, the identified Vp can be treated as a constant even though it varies between two values. As discussed earlier, the Vs decreases due to high strain and excess pore water pressure. The Vp, however, does not show significant change with time. Taking the Superstition Hill event for example (Figure 9a and 9b), the Vs drops from 140 m/s to 20 m/s due to soil liquefaction but Vp remains around 400 m/s. This observation indicates that the "apparent" constrain modulus remains linear even the shear modulus exhibits a very high nonlinearity. The reason of different nonlinear behavior in vertical and horizonal direction is explained in the following. The water can take the compression stress but cannot take the shear stress during wave propagation. Therefore, distinct nonlinear behavior is induced when propagating shear waves

(horizontal direction) and compression waves (vertical direction). In the horizontal direction, shear waves are propagated by the solid medium (i.e., skeleton of soil) and are unaffected by the water unless excessive pore water pressure is generated during the shaking. By contrast, compression waves are propagated by the soil and water in the vertical direction. Since water has higher bulk modulus than that of the soil, the vertical wave propagation is dominated by the water. Therefore, even if the horizontal direction exhibits a nonlinear behavior caused by the soil, the vertical direction still presented a linear behavior for the saturated condition (Tsai and Liu 2017; Liu and Tsai 2018).

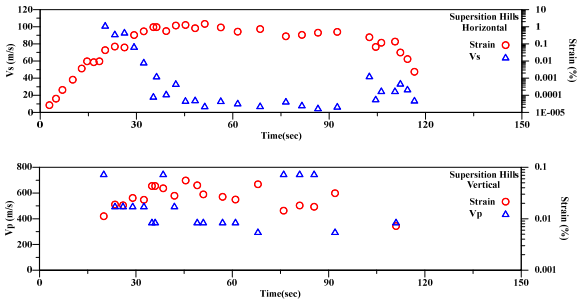

Figure 9 Comparison of identified Vs and Vp (Superstition Hill event)

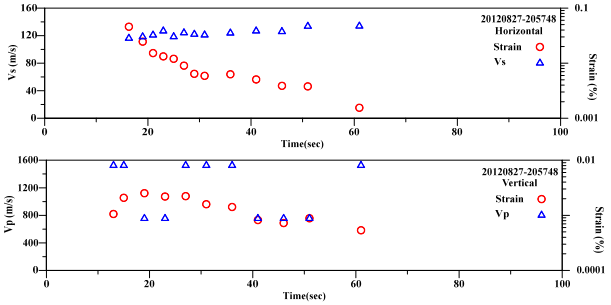

Figure 10 Comparison of identified Vs and Vp (15200401 event)

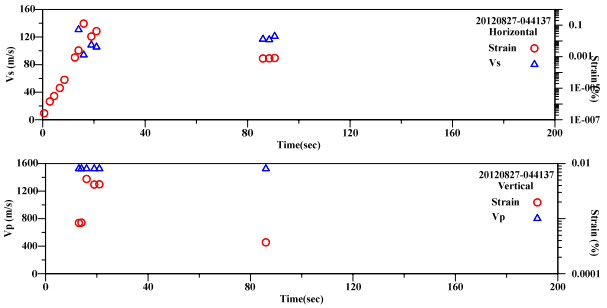

Figure 11 Comparison of identified Vs and Vp (15202921 event)

Conclusion

In this study, the Normalized Input-Output Method (NIOM) are used to identify variations in Vs and Vp using strong motions recorded at the Wildlife liquefaction array. Variations in strain development with time in different azimuthal directions are also investigated.

The identified Vs and Vp prior to strong shaking agree well with the measured Vs and Vp. The Vs decreases as the shaking level increases but the Vp remains unchanged. The different behavior is because compression waves are propagated by the soil and water in the vertical direction while shear waves are transmitted by the soil. Therefore, even soil stiffness is reduced due to large strains, the vertical wave propagation is still dominated by the water owing to its higher bulk modulus than that of the soil.

The identified threshold strain that separates whether EPWPs accumulate or not is ~0.01%. This value is consistent with the finding for sand from the small size laboratory tests. Prior to huge accumulations of EPWPs, the degradation of Vs is correlated to the magnitude of induced strain that is orientation-dependent. By contrast, as more EPWPs accumulated, EPWPs dominate the Vs degradation that is orientation-independent. Since r_u is associated with the strain level and also dominate the soil degradation, the strongest azimuth of motions is suggested to be adopted for performing 1D site response analysis. The obtained r_u based on the strongest component is more accurate and can be used for the prediction of site response for the other component.

References

[1] Haddadi, HR, Kawakami, H. (1998): Modeling Wave Propagation by using Normalized Input-Output Minimization (NIOM) Method for Multiple Linear Systems, *Doboku Gakkai Ronbunshu*, **1998b** (584), 29-39.

[2] Kishida, T., Park, DS, Sousa, R., Armstrong, R., Byon, YJ (2019): Modulus Reduction of Embankment Dams based on Downhole Array Time Series, *Earthquake Spectra*, **1**, DOI: 10.1177/101018EQS231M.

[3] Chiou, B., Darragh, R., Gregor, N., and Silva, W. (2008): NGA Project Strong-Motion Database. *Earthquake Spectra,* **24**, 23–44.

[4] Ancheta, TD, Darragh, RB, Stewart, JP, Seyhan, E., Silva, WJ, Chiou, BSJ, Wooddell, KE, Graves, RW, Kottke, AR, Boore, DM, Kishida, T. Donahue, JL (2013): PEER NGA-West2 Database. *PEER Report 2013/03*, Pacific Earthquake Engineering Research Center.

[5] Lysmer, J., Udaka, T., Tsai, CF, and Seed, HB. (1975): FLUSH A Computer Program for Approximate 3-D Analysis of Soil-Structure Interaction Problems. *Report No. EERC 75-30*, Earthquake Engineering Research Center, Berkeley, USA.

[6] Bierschwale, J. G. and Stokoe, K. H. I. (1984): Analytical evaluation of liquefaction potential of sands subjected to the 1981 Westmorland earthquake. *Geotechnical engineering report GR 84-15*, University of Texas, Austin.

[7] Vucetic, M., and Dobry, R. (1986): Pore pressure build-up and liquefaction at level sandy sites during earthquakes. *Research Rep. CE-86-3*, Dept. of Civil Engineering, Rensselaer Polytechnic Institute, Troy, NY

[8] Tsai, C. C. and Liu, H. W. (2017): Site response analysis of vertical ground motion in consideration of soil nonlinearity. *Soil Dynamics and Earthquake Engineering*,**102**, 124-136.

[9] Liu, H. W. and Tsai, C. C. (2018): Site effect of vertical motion amplification behavior observed from downhole arrays. *Journal of GeoEngineering*,**13**(1), 39-48

